



Research article



Synthesis, structure, oxygen stoichiometry, and electrical properties of doped ruddlesden-popper strontium cobaltite $\text{Sr}_{1.875}\text{Ce}_{0.025}\text{CoO}_{4-\delta}$, $\text{Sr}_{1.875}\text{Ce}_{0.025}\text{Co}_{0.75}\text{Ni}_{0.25}\text{O}_{4+\delta}$ novel compounds

Ali Shaban Abdullah^{*}, Mohammad Hicham Abazli, Manar Hassan

Chemistry Department, Faculty of Science, Tishreen University, Lattakia, Syria

ARTICLE INFO

Keywords:

Ruddlesden-popper
RP
Co-precipitation
Sol-gel
XRD
Iodometry
Electrical resistivity
Electrical capacitance
Dielectric

ABSTRACT

We report the synthesis of $\text{Sr}_{1.875}\text{Ce}_{0.025}\text{CoO}_{4-\delta}$ and $\text{Sr}_{1.875}\text{Ce}_{0.025}\text{Co}_{0.75}\text{Ni}_{0.25}\text{O}_{4+\delta}$ for the first time, each compound was synthesised using Co-precipitation and Sol-Gel methods, at 1050 °C for 144 and 120 h respectively. Oxygen stoichiometry was determined using Iodometric titration, we have noticed oxygen hypostoichiometry for Ce-doped compound and hyperstoichiometry state after Ni-doping. Electrical properties were studied for sintered pellets, Electrical resistance was measured in the range (−0.5–+0.5 v). Specific electrical resistivity and electrical conductivity were calculated from resistance measurements. It was found that the Ce-doped compound has about three times higher conductivity ($\sigma_{\text{C1}} = 0.000000058423295 \text{ s cm}^{-1}$) Compared with the Ni-doped one ($\sigma_{\text{N2}} = 0.000000022384787 \text{ s cm}^{-1}$). Electrical Capacitance was measured at 1 kHz frequency, the relative dielectric constant ϵ_r , and the loss tangent $\tan\delta$ were calculated accordingly. The results showed that the Ni-doped compound has higher capacitance but lower ϵ_r and dissipation factor values.

1. Introduction

Ruddlesden-Popper (RP) oxides of the general formula $\text{A}_2\text{BO}_{4\pm\delta}$ where A: alkaline earth metal and B: transition metal, have been one of the most investigated materials in the last two decades due to their distinguished electrical, magnetic, and optical properties. Their applications are not restricted to cathode applications in Solid Oxide Fuel Cells (SOFCs) only, but also have applications as capacitors, solar cells, and much more. These characteristic features come mainly from the layered nature of these phases [1]. There are many known unit cells related to the series, alongside a variety of distorted unit cells of the above-mentioned structures. This deformation in the structure can be predicted according to the well-known Goldschmidt tolerance factor:

$$t = \frac{r_A + r_O}{\sqrt{2}(r_B + r_O)}$$

Where r_A , r_B , and r_O are the ionic radii of the cations in A, B-sites and oxygen anion respectively. These structures are affected by the oxygen non-stoichiometry ($\pm\delta$) too [2]. However, the most widely occurrence and the highest symmetric is the T-structure with

^{*} Corresponding author.

E-mail address: ali.abdullah.academic@gmail.com (A.S. Abdullah).

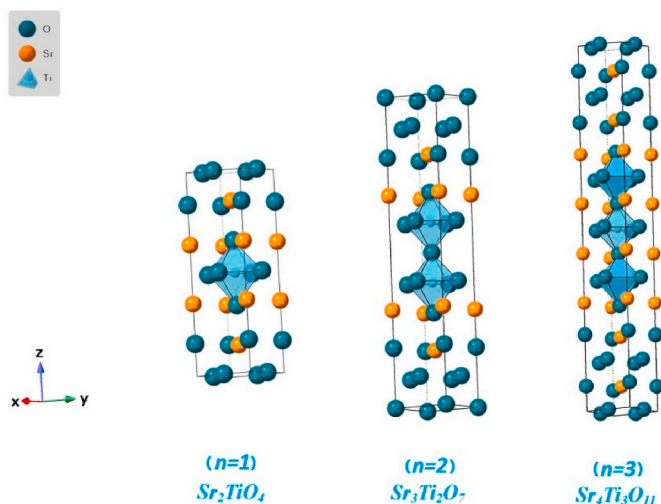


Fig. 1. Represents the first members ever [3,4] of the homologous series; the compounds Sr_2TiO_4 ($n = 1$), $Sr_3Ti_2O_7$ ($n = 2$), and $Sr_4Ti_3O_{11}$ ($n = 3$). Sketched using Crystal Maker® software.

tetragonal K_2NiF_4 -type structure and I_4/mmm space group. Its unit cell can be described as perovskite and rock-salt layers being stacked alternatively along the perpendicular axis c [3,4]. Figure (1) shows the members of the series with the general formula $A_{n+1}B_nO_{n+3}$: ($n = 1, 2, 3$).

T-structure Strontium cobaltite Sr_2CoO_4 : ($n = 1$), the first member of the homologous series, was first synthesised, doped, and characterised by Wang et al. [5]. Afterwards, a lot of papers were published about doped cobaltite, but there is no paper in the literature, as far as we know, investigating the effect of Ni or Ce-doping on the structure, oxygen non-stoichiometry, and electrical properties of the mother stoichiometric compound. Hence, the purpose of this paper. Sr_2CeO_4 is a well-known RP compound as well with a distorted unit cell (triclinic) [6] and its doped compounds have a lot of applications in the fields of photoluminescents. The Ce-doped RP compounds are known as well [7,8]. However, these papers suggest that the Ce substitution happens in the A-site rather than the B-site. There is no strontium nickelate ($n = 1, 2, 3$) that belongs to the RP series as shown by Zinkevich [9] and the only found compound with a related structure is the oxygen deficient ($n = \infty$) $SrNiO_{2.5}$. However, there are a considerable number of RP Rare Earths nickelate like the T-structure La_2NiO_4 and other related families [10,11]. There are also papers describing the effect of Ni-doping on the structures and properties of other RP families. In these papers they suggest the Ni oxidation state to be a mixture of $2+$, and $3+$ [12,13]. In this paper we investigate the effect of Ni and Ce-doping on the Strontium cobaltite structure, oxygen non-stoichiometry, and electrical properties.

2. Experimental

2.1. Synthesis process

The compounds were synthesised using two different routes [14]. However, from the same starting materials and at the same heating temperature for the same heating duration. The starting materials were: $SrCO_3$ (Merck 99.9%), $Co(NO_3)_2 \cdot 6H_2O$ (Merck 99.9%), $Ni(NO_3)_2 \cdot 6H_2O$ (Merck 99.9%), $(NH_4)_2 [Ce(NO_3)_6]$ (Merck 99.9%), Citric Acid Monohydrate. All the starting materials were weighted accurately in stoichiometric amounts and then dissolved separately in different beakers, at the least amount of deionised water, except for the insoluble strontium carbonate, it was immersed in deionised water then concentrated nitric acid (65%) was poured, drop by drop from a fixed burette while a magnetic stirrer stirred the solution until all the carbonate decomposed and the CO_2 releasing stopped. Afterwards, the concentrated solutions of the other nitrate were poured over one by one to achieve homogeneity (citric acid solution of molar ratio 1.5:1 for every metal cation was added to sol-gel samples only for the purpose of forming the gel). The mixture was heated on a hot plate while stirring at $100^\circ C$ until the total evaporation of the solvent and the total precipitation of nitrate crystals. That is for co-precipitation samples, the same steps were applied for sol-gel samples. After solution evaporation, pink gel was formed. Afterwards, samples were dried in an electrical oven at $100^\circ C$ for 2 h. Afterwards, the precipitates of the co-precipitation method were grounded in an agate mortar into a fine coloured powder. As for the sol-gel method, the gel was placed in a crucible and then heat treated on benzene torch for 30 min until the flash point. Afterwards, the co-precipitation precipitates were heat treated to decompose the nitrate until the releasing of NO_2 stopped, then the residues of each method were grounded again to a fine black powder, then placed in a muffle furnace at $700^\circ C$ for 2 h then at $900^\circ C$ for another 2 h to decompose all the remaining undecomposed nitrate to give the matching oxides, the samples then re-grounded once more and pressed at 4 metric tons using a Carver hydraulic press to give pellets. The pellets were sintered at $1050^\circ C$ for 144 h and 120 h, for Ce-doped and Ni,Ce-doped compounds respectively. Novel $Sr_{1.875}Ce_{0.025}CoO_{3.96}$ and $Sr_{1.875}Ce_{0.025}Co_{0.75}Ni_{0.25}O_{4.22}$ compounds are hereafter, designated C1, N2 respectively.

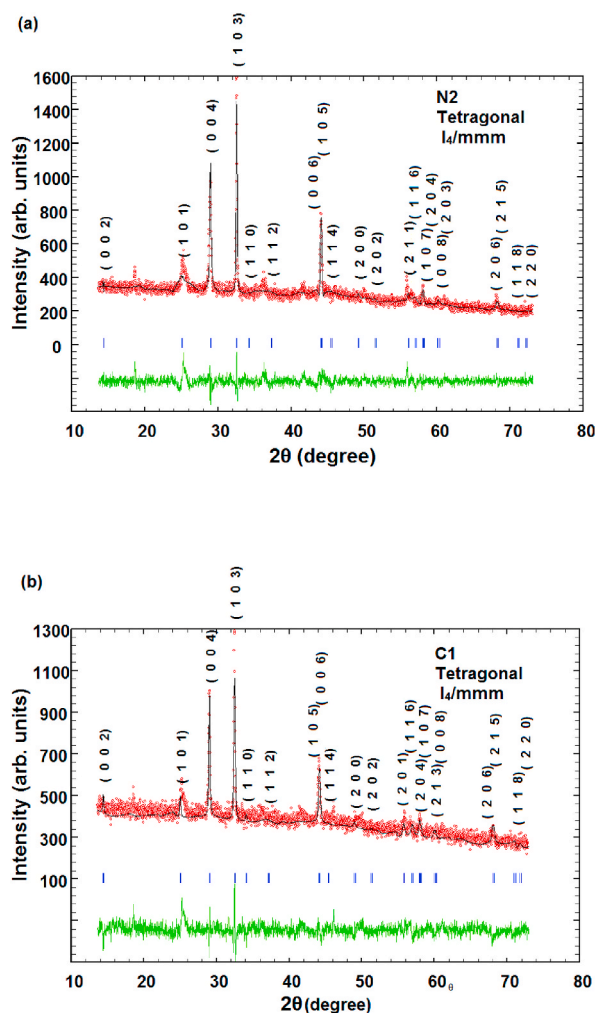


Fig. 2. Resembles the Rietveld refinement process for (a) N2 and (b) C1 compounds. Red dots are the observed data, the solid black line is the calculated data, the solid green line is $I_{\text{obs}} - I_{\text{cal}}$ and the blue dashes are Bragg positions where miller indices of the tetragonal phase are shown in both patterns.

2.1.1. Structure determination

The fine powders of the synthesised compounds were characterised using a (Philips pw 1840) X-ray diffractometer equipped with a $\text{Cu K}\alpha$ source at room temperature. The Rietveld refinement process was performed using Fullprof software® to determine the room temperature phase, cell parameters, atomic coordinates, bond lengths and electron density, then crystallite size and lattice strains were calculated using the Sherrer equation using PANalytical X'pert Highscore plus® version 3.00.

2.2. Iodometric titration

The oxygen stoichiometry was determined using iodometric titration from analytical-grade materials as described by K. Conder et al. [15] but with alteration in the solution concentration and sample weights; the starch indicator (Merck) was prepared first by dissolving 0.8 g in 100 ml double-distilled water. Afterwards, 1 M HCl (Merck 37%), 2 M KI (Riedel-de Haën 99%), and 0.05 M $\text{Na}_2\text{S}_2\text{O}_3$ (Tekim 99%) solutions were prepared using double-distilled water and used in an instant. Firstly, 0.21 g of greyish-black C1 and N2 respectively were weighed accurately and then each weight was dissolved in 25 ml of 1 M HCl Solution to obtain a brownish-red homogeneous solution, then 3 ml of 2 M KI solution was added to the mixture to obtain a golden-yellow colour. The solutions were titrated against a 0.05 M Sodium Thiosulphate solution, then the starch indicator was added near the endpoint, giving the solutions a brownish-yellow colour, then the titration ended with a pink colour. The titration was repeated three times for each sample.

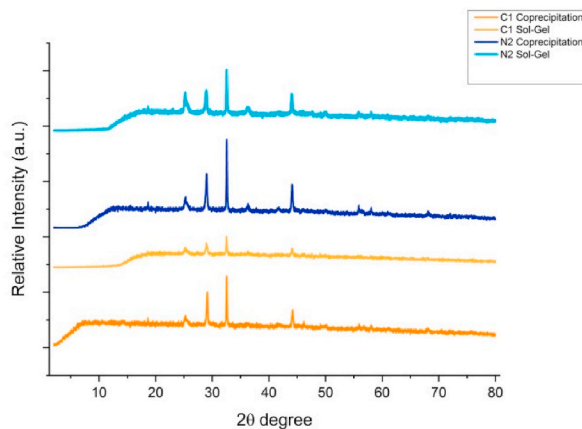


Fig. 3. Shows the experimental XRD patterns of the synthesised compounds.

Table 1

Shows cell parameters, average crystallite size and lattice strain for C1, N2, and two other compounds for comparison.

Compound	Chemical formula	a°	c A°	D (nm) average	Lattice strain%
Mother phase [5]	Sr ₂ CoO ₄	3.75	12.33	–	–
Well-known compound [16]	SrLaCoO ₄	3.806	12.5	–	–
C1 Co-precipitation	Sr _{1.875} Ce _{0.025} CoO _{3.96}	3.71938	12.2999	30.975	0.448125
C1 Sol-Gel	Sr _{1.875} Ce _{0.025} CoO _{3.96}	3.70297	12.2991	25.1625	0.586875
N2 Co-precipitation	Sr _{1.875} Ce _{0.025} Co _{0.75} Ni _{0.25} O _{4.22}	3.70231	12.3151	41.333	0.3878
N2 Sol-Gel	Sr _{1.875} Ce _{0.025} Co _{0.75} Ni _{0.25} O _{4.22}	3.7048	12.3712	32.444	0.3443

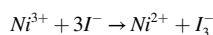
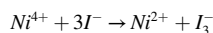
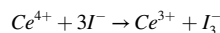
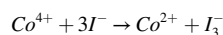
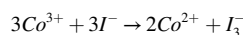
2.3. Electrical resistivity and capacitance measurements

The samples of C1 and N2 were pressed using a hydraulic press at 4 metric tons, then the two pellets were sintered at 1050° c for 3 h. Afterwards, the pellet's diameter and width were measured using a manual Vernier caliper. Two props with 1 mm spacing were applied on the pellet surfaces, then Direct Current (DC) voltage between the props was altered in the range (–0.5v - +0.5v) and the flowing of the Direct Current was measured accordingly. The Capacitance was measured at 1 kHz frequency.

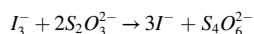
3. Results and discussion

3.1. Oxygen nonstoichiometry

The oxygen nonstoichiometry is calculated from the results of iodometric titration, which has a very good reproducibility and accuracy [15]; the following Redox reactions are thought to take place during the process.



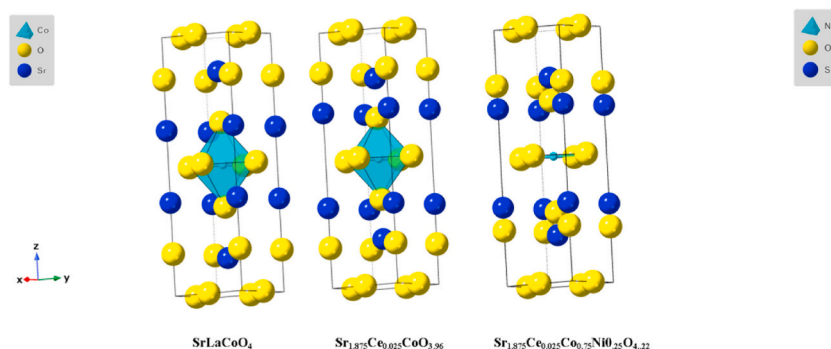
The oxygen content can be calculated from the liberated amount of Iodine with the titration against Sodium Thiosulphate solution.



In the titration, the Strontium cation valence is assumed to be 2+ and Cerium cation to be 4+. The results of iodometry show that the C1 compound is hypostoichiometric $-\delta = 0.04$ and the N2 compound is hyperstoichiometric $+\delta = 0.22$.

Table 2shows the atomic coordinates of synthesised C1, N2 compounds and SrLaCoO₄ compound.

SrLaCoO ₄ [16]		x	y	z
	Co	0	0	0
	Sr/La	0	0	0.361
	Oeq	0	0.5	0
	Oap	0	0	0.163
Sr _{1.875} Ce _{0.025} CoO _{3.96}	Co	0	0	0
	Sr/Ce	0	0	0.31442
	Oeq	0	0.5	0
	Oap	0	0	0.15774
Sr _{1.875} Ce _{0.025} Co _{0.75} Ni _{0.25} O _{4.22}	Co/Ni	0	0	0
	Sr/Ce	0	0	0.30777
	Oeq	0	0.5	0
	Oap	0	0	0.21787

**Fig. 4.** Represents the effect of Ce-doping (compound Sr_{1.875}Ce_{0.025}CoO_{3.96}), and Ce, Ni-doping (compound Sr_{1.875}Ce_{0.025}Co_{0.75}Ni_{0.25}O_{4.22}) in contrast with SrLaCoO₄.**Table 3**

Represents the calculated bond lengths for C1 and N2 compounds.

Compound	C1	N2
Co/Ni-O _{eq} (× 4)	1.85969 Å	1.85116 Å
Co/Ni-O _{ap} (× 2)	1.94019 Å	2.68309 Å
Sr/Ce-O _{eq} (× 4)	2.94429 Å	3.00517 Å
Sr/Ce-O _{ap} (× 4)	2.65220 Å	2.63690 Å
Sr/Ce-O _{ap} (× 1)	1.92715 Å	1.10713 Å

4. Structural study

Figure (2) shows the Rietveld refinement process for N2 compound, figure(2-a), and for C1 compound, figure(2-b), using Fullprof software. We got an acceptable fit for the proposed model (χ^2 for C1: 2.2 and for N2: 1.54). The atomic positions were taken from the structural model of the compound SrLaCoO₄ (COD ID: 1008258) of the same space group and structure [16]. According to the refinement process, the space group, atomic coordinates, and cell parameters were concluded and is shown in Table 1. Afterwards, electron density maps and bond lengths were calculated using fullprof suit. The crystallite size, and lattice strains were calculated using PANalytical X'pert Highscore plus version 3.00. Figure (3) shows the XRD patterns for the synthesised compounds. From the experimental and calculated data and according to the proposed model, the compounds found to be of the tetragonal system and to have I₄/mmm symmetry. We have noticed a minor shrinkage in cell parameters a, b, and c for both newly synthesised compounds in contrast with other related compound, Table 1 shows the cell parameters of the three compounds. We attribute the shrinking in cell parameters to the small cationic radius (all ionic radius were taken from Shannon [17]) of Ce⁴⁺ ($Ce_{VI}^{4+} = 0.87 \text{ \AA}$, $Ce_X^{4+} = 1.07 \text{ \AA}$), which concludes that the Ce-doping process is being happening in the A-site rather than the B-site ($Sr_{IX}^{2+} = 1.31 \text{ \AA}$, $Co_{VI}^{4+} = 0.53 \text{ \AA}$). Otherwise, the cell parameters would be elongated. As for the Ce,Ni-doped compound a likewise shrinking in cell parameters

was noticed. The similarity in cell parameters for both C1 and N2 compounds can be attributed to the similarity in ionic radius between Co⁴⁺ and Ni ($Ni_{VI}^{4+} = 0.48 \text{ \AA}$, $Ni_{VI}^{3+} = 0.60 \text{ \AA}$ for high-spin state, and $Ni_{VI}^{3+} = 0.56 \text{ \AA}$ for low-spin state) cations, which leads to a conclusion that Ni valence state is an in-between valence state. However, the oxygen stoichiometry titration results for both samples prefer the 4+ valence state; the Ce-doping process leads to a hypostoichiometry situation, that is because the doping amount is rather small so that the new compound does not have many interstitial spaces for the oxygen anions to occupy them. However, in the Ni-

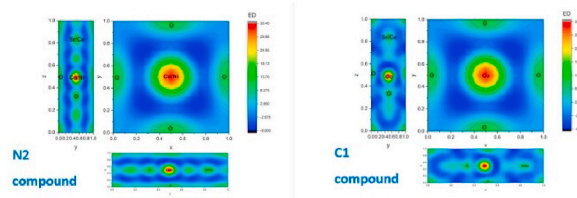


Fig. 5. Shows the calculated electron density maps (Fourier maps) for C1 (right) and N2 (left) compounds.

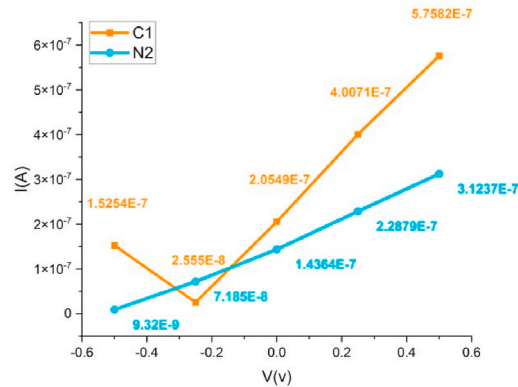


Fig. 6. Shows Direct Current (DC) vs. Voltage measurements for sintered pellets of C1 and N2 compounds.

doping situation, an oxygen hyperstoichiometry was noticed. Which leads to the conclusion that there are interstitial spaces enough for the oxygen anions to occupy them, that is because of the relatively high doping amount of the Ni cation at the first hand and the small cationic radius of the Ni cation at the second hand, which only can be found in the 4+ valence state. Another notable observation of the studied compounds is the atomic position shifts in contrast with the compound SrLaCoO₄. Table 2.

The atomic coordinates of C1 and SrLaCoO₄ are very similar with minor shifts due to the small cationic radius of Ce⁴⁺ cation as mentioned earlier. However, in N2 case, we notice a major shift in the apical oxygen, figure (4). That is attributed to the distorted nature of the Ni⁴⁺ cation at the 6-coordinated site, which is noticed in the calculated bond lengths as well, Table 3, the bond lengths between Co and apical Oxygens are: 1.94019 Å, 2.68309 Å for C1 and N2 compounds respectively.

The elongation of Co–O bond length is then attributed to Ni cations being replaced in the Co-site causing them to distort the perfect octahedra to an elongate one along the z axis. The distortion is noticed in the calculated electron density maps (Fourier mapping), figure(5).

4.1. Electrical resistivity and capacitance

4.1.1. Electrical resistance and resistivity

The electrical resistance to DC flowing was measured for C1 and N2 sintered pellets in the range (–0.5 - +0.5 v), figure (6), by dividing the voltage difference between the two props and the flowing current according to ohm’s law:

$$R = \frac{U}{I} \tag{1}$$

The electrical resistivity to DC flowing was calculated accordingly according to Ref. [18]:

$$\rho = R \frac{A}{d} \tag{2}$$

Where:

d is the pellets thickness; (d_{C1}: 0.2 cm and d_{N2}: 0.14 cm).

A is the surface area:

$$A = \pi r^2; \tag{3}$$

r is pellets’ radii; (r_{C1}: 1.12 cm and r_{N2}: 1.115 cm).

The electrical conductivity of the Direct Current (DC) was calculated accordingly by:

Table 4

Shows the electrical properties of C1 and N2 compounds in SI units.

properties	R (Ω)	$\rho(\Omega/\text{cm})$	$\sigma(\text{S}/\text{cm})$	C (pF)	ϵ_r	$\tan\delta$
C1	0.87×10^6	1.71×10^7	5.84×10^{-8}	700	401	26.17×10^{-4}
N2	1.6×10^6	4.46×10^7	2.23×10^{-8}	800	324	12.42×10^{-4}

$$\sigma = \frac{1}{\rho} \quad (4)$$

The ratio $\sigma_{\text{C1}}/\sigma_{\text{N2}} = 2.60$ indicates that the electrical conductivity was dropped by approximately 3 times less after Ni-doping.

4.1.2. Electrical capacitance measurement

The relative dielectric constant was calculated according to Ref. [18]:

$$\epsilon_r = 11.3 \times 10^{12} \cdot C \frac{\text{d}}{\text{A}} \quad (5)$$

The relative dielectric constant is a measure of a material's ability to polarise in the presence of an electric field and to store the electrostatic energy in the material. Table 4 shows the electrical properties of C1 and N2 compounds.

The novel compounds show relatively high relative dielectric constant values in comparison with other RP: (n = 1) oxides. The relative dielectric constant of N2 and C1 compounds is about 10 times greater than that of the Sr_2TiO_4 compound [19] at the same conditions (at room temperature and at 1 kHz frequency).

The loss angle tangent is a measurement resembling the dissipated amount of energy in the dielectric [18].

The loss angle tangent was calculated by:

$$\tan \delta = \frac{1}{\rho \cdot \omega \cdot \epsilon_0 \cdot \epsilon_r}; \quad (6)$$

$$\omega = 2 \cdot \pi \cdot f; \quad (7)$$

f is the frequency ($f = 1$ kHz).

The lower loss tangent value is the lower the loss of the stored energy in the dielectric.

5. Conclusion

- Two novel Ruddlesden-Popper compounds: $\text{Sr}_{1.875}\text{Ce}_{0.025}\text{CoO}_{4-\delta}$, $\text{Sr}_{1.875}\text{Ce}_{0.025}\text{Co}_{0.75}\text{Ni}_{0.25}\text{O}_{4+\delta}$ were synthesised using two different routes.
- The Sol-Gel route is a better method for synthesising RP compounds because of the smaller crystallite size in contrast with the Co-precipitation route at the same heating temperature for the same heating duration.
- The Ni-doping process resulted a considerable accommodation of oxygen anions ($\Delta\delta = 0.26$).
- Structural study revealed a rather considerable shift in apical oxygen position after Ni-doping owing to the deformation in B-site octahedra in the form of elongation in the z direction.
- The Ce-doped compound has better electrical properties than the Ce, Ni-doped compound.

6. Recommendations

We recommend a more comprehensive study of the electrical properties of these new oxides in order to obtain a deeper understanding of their electrical conductivity mechanism.

Author contribution statement

Ali Shaban Abdullah: Conceived and designed the experiments; Performed the experiments; Analyzed and interpreted the data; Contributed reagents, materials, analysis tools or data; Wrote the paper.

Mohammad Hicham Abazli, Manar Hassan: Analyzed and interpreted the data.

Data availability statement

Data included in article/supplementary material/referenced in article.

Declaration of competing interest

The authors declare that they have no known competing financial interests or personal relationships that could have appeared to

influence the work reported in this paper.

References

- [1] G. Nirala, D. Yadav, S. Upadhyay, Ruddlesden-Popper phase A_2BO_4 oxides: recent studies on structure, electrical, dielectric, and optical properties, *J. Adv. Ceram.* 9 (2020) 129–148, <https://doi.org/10.1007/s40145-020-0365-x>.
- [2] I.B. Sharma, D. Singh, Solid state chemistry of Ruddlesden-Popper type complex oxides, *Bull. Mater. Sci.* 21 (1998) 363–374.
- [3] S.N. Ruddlesden, P. Popper, New compounds of the K_2NiF_4 type, *Acta Crystallogr.* 10 (8) (1957) 538–539.
- [4] S.N. Ruddlesden, P. Popper, The compound $Sr_3Ti_2O_7$ and its structure, *Acta Crystallogr.* 11 (1) (1958) 54–55.
- [5] X.L. Wang, H. Sakurai, E. Takayama-Muromachi, Synthesis, structures, and magnetic properties of novel Ruddlesden–Popper homologous series $Sr_{n+1}Co_nO_{3n+1}$ ($n=1, 2, 3, 4, \text{ and } \infty$), *J. Appl. Phys.* 97 (10) (2005) 10M519.
- [6] L.A. Rocha, M.A. Schiavon, C.S. Nascimento Jr., L. Guimaraes, M.S. Goes, A.M. Pires, J.L. Ferrari, Sr_2CeO_4 : electronic and structural properties, *J. Alloys Compd.* 608 (2014) 73–78.
- [7] V.N. Chaudhari, A.P. Khandale, S.S. Bhoga, Synthesis and characterization of Ce-doped $Sm_2CuO_{4+\delta}$ cathode for IT-SOFC applications, *Ionics* 23 (2017) 2553–2560.
- [8] A.P. Khandale, S.S. Bhoga, Electrochemical performance of $Nd_{1-x}Ce_xCuO_{4\pm\delta}$ mixed-ionic–electronic conductor for intermediate solid oxide fuel cells, *Solid State Ionics* 182 (1) (2011) 82–90.
- [9] M. Zinkevich, Constitution of the Sr–Ni–O system, *J. Solid State Chem.* 178 (9) (2005) 2818–2824.
- [10] G. Amow, I.J. Davidson, S.J. Skinner, A comparative study of the Ruddlesden-Popper series, $La_{n+1}Ni_nO_{3n+1}$ ($n=1, 2$ and 3), for solid-oxide fuel-cell cathode applications, *Solid State Ionics* 177 (13–14) (2006) 1205–1210.
- [11] J.H.D. Araujo, P.M. Pimentel, R.M.P.B. Oliveira, F.S. Oliveira, O.R. Bagnato, D.M.D.A. Melo, Synthesis and Structural Characterization of Sm–SrNickelates, 2012.
- [12] N. Kieda, S. Nishiyama, K. Shinozaki, N. Mizutani, Nonstoichiometry and electrical properties of La_2CuO_4 and $La_2(Cu, Ni)O_4$, *Solid State Ionics* 49 (1991) 85–88.
- [13] A.P. Khandale, S.S. Bhoga, R.V. Kumar, Effect of Ni doping on structural, electrical and electrochemical properties of $Nd_{1-x}Ce_xCu_{1-x}Ni_xO_{4+\delta}$ mixed ionic–electronic conductor, *Solid State Ionics* 238 (2013) 1–6.
- [14] V.S. Shinde, S.G. Dahotre, Comparative study of structural and magnetic properties of Ni and La substituted calcium hexaferrite, *Cerâmica* 67 (2021) 301–307.
- [15] K. Conder, E. Pomjakushina, A. Soldatov, E. Mitberg, Oxygen content determination in perovskite-type cobaltates, *Mater. Res. Bull.* 40 (2) (2005) 257–263.
- [16] G. Demazeau, C. Ph. G. Le Flem, M. Pouchard, P. Hagenmuller, J.L. Soubeyrou, A.G. Robins, Propriétés structurales et magnétiques de $SrLaCoO_4$: une discussion de la structure électronique du cobalt trivalent, *New J. Chem.* 3 (3) (1979) 171–174.
- [17] R.D. Shannon, Revised effective ionic radii and systematic studies of interatomic distances in halides and chalcogenides, *Acta Crystallogr. Sect. A Cryst. Phys. Diffr. Theor. Gen. Crystallogr.* 32 (5) (1976) 751–767.
- [18] R.H. Saleh, M. Deeb, Study of electrical properties of cobalt oxide-doped sodium meta vanadate at different frequencies, *Heliyon* 8 (9) (2022), e10471.
- [19] W. Ge, C. Zhu, H. An, Z. Li, G. Tang, D. Hou, Sol–gel synthesis and dielectric properties of Ruddlesden–Popper phase $Sr_{n+1}Ti_nO_{3n+1}$ ($n=1, 2, 3, \infty$), *Ceram. Int.* 40 (1) (2014) 1569–1574.